^{31}P MAS-NMR of Crystalline Phosphorous Sulfides. Correlation of
^{31}P Chemical Shielding Tensors with Local Environments

by

Hellmut Eckert, Cheryl S. Liang, Galen D. Stucky

Department of Chemistry
University of California
Santa Barbara, California 93106

Abstract

^{31}P MAS NMR is used to characterize local phosphorus environments in $-P_4S_3$, P_4S_7, P_4S_9, and P_4S_{10}. MAS-NMR spectra of P_4S_3 enable a chemical shift discrimination of the apical P atoms belonging to the two crystallographically distinct molecules in the unit cell. No line narrowing is observed for the basal P-atoms, indicating reorientation of the molecules about their C_3 axes, as previously suggested from neutron diffraction data. MAS-NMR spectra of P_4S_7 show distinct resonances for all four crystallographically inequivalent P atoms within the molecular P_4S_7 units. Since, due to these site inequivalencies, spin-spin couplings are observable (contrary to liquid state NMR), chemical shift assignments to P-P bonded units and $S=PS_{3/2}$ groups are possible. The spectra of P_4S_9 and P_4S_{10} disagree with earlier literature reports, and are subject to a reinterpretation in the present study. Analyses of spinning sideband intensities yield the principal shielding tensor components, which are correlated with crystallographic data. $S=PS_{3/2}$ and $PS_{3/2}$ units are easily distinguished by opposite signs of the chemical shift anisotropies. In P_4S_3 and P_4S_{10}, where these units have point symmetries close to C_{3v}, the chemical shift tensors are close to axially symmetric, whereas the more strongly distorted units in P_4S_7 and P_4S_9 are characterized by sizeable asymmetry parameters. The latter quantity is proposed to be a sensitive measure of the range of S-P-S bonding angles within the cage units. However, for both $S=PS_{3/2}$ and $PS_{3/2}$ microstructures, such distortions mainly affect the most deshielded components ∂_{33}, whereas the most shielded components ∂_{11} remain essentially unchanged. Regardless of their detailed local symmetries, $S=PS_{3/2}$ and $PS_{3/2}$ units are easily distinguished by ∂_{11} components of -50 and 0 ppm, respectively. These results illustrate the advantage of anisotropic over isotropic chemical shift information as a diagnostic tool for the identification of microstructures, and suggests the utility of this approach in the structural analysis of disordered systems.

1

AD A196557

REPORT DOCUMENTATION PAGE	READ INSTRUCTIONS BEFORE COMPLETING FORM

1. REPORT NUMBER	2. GOVT ACCESSION NO.	3. RECIPIENT'S CATALOG NUMBER
16		

4. TITLE (and Subtitle)	5. TYPE OF REPORT & PERIOD COVERED
31_p MAS-NMR of Crystalline Phosphorous Sulfides. Correlation of 31_p Chemical Shielding Tensors with Locql Environments.	Technical
	6. PERFORMING ORG. REPORT NUMBER

7. AUTHOR(s)	8. CONTRACT OR GRANT NUMBER(s)
Hellmut Eckert, Cheryl S. Liang, Galen D. Stucky	N00014-87-K-0457

9. PERFORMING ORGANIZATION NAME AND ADDRESS	10. PROGRAM ELEMENT, PROJECT, TASK AREA & WORK UNIT NUMBERS

11. CONTROLLING OFFICE NAME AND ADDRESS	12. REPORT DATE
	May 1988
	13. NUMBER OF PAGES

14. MONITORING AGENCY NAME & ADDRESS(If different from Controlling Office)	15. SECURITY CLASS. (of this report)
	Unclassified
	15a. DECLASSIFICATION/ DOWNGRADING SCHEDULE

16. DISTRIBUTION STATEMENT (of this Report)

17. DISTRIBUTION STATEMENT (of the abstract entered in Block 20, if different from Report)

18. SUPPLEMENTARY NOTES

Submitted for publication to: Journal of Physical Chemistry

19. KEY WORDS (Continue on reverse side if necessary and identify by block number)

NMR, phosphorous sulfides, zeolites, disorder

20. ABSTRACT (Continue on reverse side if necessary and identify by block number)

DD FORM 1473 EDITION OF 1 NOV 68 IS OBSOLETE
1 JAN 73
S/N 0102-LF-014-6601

^{31}P MAS-NMR of Crystalline Phosphorus Sulfides. Correlation of ^{31}P Chemical Shielding Tensors with Local Environments.

Hellmut Eckert, Cheryl S. Liang, and Galen D. Stucky

Department of Chemistry
University of California at Santa Barbara
Goleta CA 93106

Abstract

^{31}P MAS NMR is used to characterize local phosphorus environments in α-P_4S_3, P_4S_7, P_4S_9, and P_4S_{10}. MAS-NMR spectra of α-P_4S_3 enable a chemical shift discrimination of the apical P atoms belonging to the two crystallographically distinct molecules in the unit cell. No line narrowing is observed for the basal P-atoms, indicating reorientation of the molecules about their C_{3v} axes, as previously suggested from neutron diffraction data. MAS-NMR spectra of P_4S_7 show distinct resonances for all four crystallographically inequivalent P atoms within the molecular P_4S_7 units. Since, due to these site inequivalencies, spin-spin couplings are observable (contrary to liquid state NMR), chemical shift assignments to P-P bonded units and $S=PS_{3/2}$ groups are possible. The spectra of P_4S_9 and P_4S_{10} disagree with earlier literature reports, and are subject to a reinterpretation in the present study. Analyses of spinning sideband intensities yield the principal shielding tensor components, which are correlated with crystallographic data. $S=PS_{3/2}$ and $PS_{3/2}$ units are easily distinguished by opposite signs of the chemical shift anisotropies. In P_4S_3 and P_4S_{10}, where these units have point symmetries close to C_{3v}, the chemical shift tensors are axially symmetric, whereas the more strongly distorted units in P_4S_7 and P_4S_9 are characterized by sizeable asymmetry parameters. The latter quantity is proposed to be a sensitive measure of the range of S-P-S bonding angles within the cage units. However, for both $S=PS_{3/2}$ and $PS_{3/2}$ microstructures, such distortions mainly affect the most deshielded components ∂_{33}, whereas the most shielded components ∂_{11} remain

essentially unchanged. Regardless of their detailed local symmetries, $S=PS_{3/2}$ and $PS_{3/2}$ units are easily distinguished by ∂_{11} components of -50 and 0 ppm, respectively. These results illustrate the advantage of anisotropic over isotropic chemical shift information as a diagnostic tool for the identification of microstructures, and suggests the utility of this approach in the structural analysis of disordered systems.

Introduction

While the Phosphorus-Sulfur system has been attractive to investigators for many decades,[1-4] it has been only recently that phosphorus sulfides have gained substantial interest in materials science. Phosphorus chalcogenides are important constituents of many non-oxide chalcogenide glasses, whose infrared transmitting properties offer new opportunities for optical waveguide applications. Furthermore, lithium containing glasses based on phosphorus and silicon sulfides appear promising candidates for solid electrolytes in low-equivalent weight batteries.[5] The structural elucidation of such disordered systems, which may provide useful guidelines for tailoring physicochemical properties in these systems requires (a) techniques that are not inherently limited by the lack of periodicity, such as solid state NMR[6], and (b) parallel applications of such techniques to crystalline model compounds with well-known nearest neighbor environments. Binary *phosphorus sulfides are ideal model systems for such glasses,* because many stoichiometric compounds, P_4S_3, P_4S_4, P_4S_5, P_4S_7, P_4S_9, and P_4S_{10}, are known, hence providing the opportunity of studying a considerable variety of phosphorus-chalcogen environments, all of which may occur in chalcogenide glasses. The crystal structures of all of these compounds are well-established,[7-12] thus permitting detailed correlations of the solid state NMR characteristics with the local phosphorus environments. All of the compounds in question have been characterized previously by liquid state NMR,[13-18] and, in addition, several solid state NMR studies have been published,[19-28] but very little interpretation has been given. Furthermore, previous solid state NMR studies have concentrated on isotropic chemical shift measurements, in spite of the fact that it is frequently the anisotropic information, that can be connected most directly with structural information. Such information is available from the spinning sideband patterns obtained under conditions of slow magic angle spinning.[29,30] The objective of the present study is to investigate the suitability of ^{31}P MAS NMR to distinguish between different local phosphorus

environments that may occur in non-oxide glasses. To this end, the the ^{31}P chemical shielding properties in P_4S_3, P_4S_7, P_4S_9, and P_4S_{10}, (see Figure 1) have been are studied and discussed in terms of the known crystal structures of these compounds. These results are intended to serve as benchmark data for the structural analysis of non-crystalline phosphorus chalcogenide systems.

Experimental

<u>Sample Preparation and Characterization</u>

The syntheses followed published procedures, and the identity and purity of the compounds was verified by x-ray powder diffraction, differential scanning calorimetry (using a Dupont 912 analyzer), and by liquid state ^{31}P NMR. All sample manipulations were carried out in an Argon-filled dry box. P_4S_3 was obtained from Strem Chemicals and recrystallized from dried CS_2, mp. 165-171 °C (lit. 173). P_4S_7 and P_4S_9 were obtained from the elements in a molar ratio of 4:8.5, heated in vacuo at 500°C for 100 hours. Following the procedure outlined in ref. 31 the product was subsequently refluxed in CS_2, leaving a residue whose elemental analysis yielded a stoichiometry $P_4S_{6.8}$, mp. 305-309 °C (lit. 307.5-308). The supernatant solution consists of pure P_4S_9, as verified by liquid state NMR. After solvent evaporation , the material was recrystallized from CS_2 to yield yellow crystals, mp. 248-267 °C (lit. 240-270). Differential scanning calorimetry and X-ray powder diffraction indicate that of the two known modifications of P_4S_9, only the disordered phase, labeled P_4S_9-I in ref. 31, was present. P_4S_{10} was obtained commercially from Eastman Kodak. Previous studies have shown that commercial "P_4S_{10}" is actually a mixture of P_4S_9, P_4S_{10}, and S_8,[15,32] and our material was no exception. Following the procedure outlined in ref. 15, we Soxhlet-extracted the commercial product twice with CS_2. The solid formed after solvent evaporation was subsequently recrystallized from CS_2; mp. 287-295 °C (lit. 287-288).

NMR Studies. Solid State NMR studies were carried out at 121.65 MHz on a General Electric GN 300 widebore system, equipped with a high power magic-angle spinning probe from Doty Scientific. Samples were spun within sapphire spinners of 7mm o.d. at speeds between 3.5 and 5.5 kHz. Additional experiments were carried out at 202.49 MHz on a Bruker AM 500 spectrometer system, available at the Southern California Regional NMR Facility at Caltech, using a high-speed multinuclear probe from Doty Scientific (typical spinning speeds 5-7 kHz in 5mm sapphire spinners). To avoid hydrolysis by

atmospheric moisture, the spinners were sealed with a thin layer of high-vacuum grease, and spun with evaporated liquid nitrogen. Standard single-pulse acquisition (90° pulse lengths 7μs at 121.65 MHz, 4 μs at 202.49 MHz) was used. Recycle delays of 3-10 minutes were typically sufficient to yield spectra free from saturation effects. Chemical shift tensor components were extracted from typically 8 spinning sideband intensities, using the graphical procedure of Herzfeld and Berger.[30] Unless noted specifically, agreement of the shift tensor components was typically within ±5 ppm for the two different field strengths used. All values are referenced against external liquid H_3PO_4 (downfield shifts positive).

Results, Assignments, and Interpretation

Table 1 summarizes the chemical shift tensor components, the isotropic chemical shifts ∂_{iso}, obtained from the centerband frequencies, and the asymmetry parameter $\eta = (\partial_{22}-\partial_{11})/(\partial_{33}-\partial_{22})$ for the compounds under study. The spectra of the individual compounds are shown in Figures 2-6, and are discussed in the following within the context of the crystallographic information available.

$\underline{P_4S_3}$. P_4S_3 is known to undergo a first-order phase transition at 314 K from a rigid molecular structure (α-P_4S_3) to a plastic crystalline phase (β-P_4S_3) at 314 K. Our investigations on β-P_4S_3 agree with those in the literature[19-21] and are not repeated here. Previous solid state NMR studies of α-P_4S_3, carried out with multiple-pulse line-narrowing[25] were able to distinguish between the apical and basal P atoms. However, the crystal structure is known to contain two crystallographically inequivalent molecules in the unit cell, which were not resolved in this previous work. As shown in Figure 2, such site discrimination is easily possible using magic-angle spinning NMR. Spectra obtained at two different field strengths confirm the presence of two singlets in a 1:1 ratio. Both peaks are assigned to apical P atoms of the two crystallographically distinct P_4S_3 molecules, on the basis of their isotropic chemical shifts as well as the near-axial symmetry of the shielding tensors reflected in the spinning sideband patterns. The chemical shift tensor components found for those individual sites agree well with the average values reported in references 25 and 27. Table 1 shows that although both chemical shift tensors assigned to the apical P atoms are close to axially symmetric, there is a significant difference between the asymmetry parameters. The crystal structure of α-P_4S_3 reveals that the local environments of the apical P atoms, although fairly close to the ideal C_{3v} symmetry, are nevertheless subject to slight distortions.[8] Here, and in the discussion to follow, we will use the range Δ over which the S-P-S

bond angles within the molecular cages vary, as a convenient measure of such distortions. Since the deviation from axial symmetry of the chemical shift tensor is expected to increase with the extent of these symmetry distortions, we assign the resonance with the higher asymmetry parameter to the site with the wider range of S-P-S bond angles. Thus, the peak centered at 91.0 ppm is assigned to the P(4) site, and that at 84.5 ppm to the more symmetric P(4') site (using the nomenclature of reference 5). The apical P atoms are most deshielded in the direction of the C_3 axis.

Surprisingly, and in contrast to the liquid state NMR spectrum, the solid state NMR spectrum of the ß-phase, and the multiple-pulse study of the - phase[25], no sharp signals assignable to the basal phosphorus atoms are observed in our room-temperature MAS-NMR study. This result is significant in view of a recent re-investigation of the crystal structure by x-ray and neutron diffraction, which suggests that the average vibrational amplitude of the apical P atom is significantly less than that of the basal P atoms[11] at room temperature. As pointed out in that study, this result suggests the occurrence of reorientational jumps of the P_4S_3 molecules about their C_3 axes in P_4S_3 as this compound approaches the phase transition to the ß- phase at 314 K. The MAS-NMR spectrum confirms this interpretation. Inspection of Figure 2 shows that the spinning sideband patterns arising from the apical P-atoms are superimposed upon a broad spectral feature not narrowed by magic-angle spinning. As a result of these jumps, the transverse magnetization of individual spin-packets is not refocused after a full rotor cycle, and thus no line-narrowing can be achieved.

P_4S_{10}. The spectrum of P_4S_{10}, shown in Figure 3, differs substantially from previous MAS-NMR results[22,23,25], where only a single sharp resonance was observed. The present result, which agrees with an earlier low-field wideline NMR study[27], reveals that P_4S_{10} has a sizeable chemical shift anisotropy, with an essentially axially symmetric shielding tensor, as expected from the near-perfect C_{3v} symmetry of the $S=PS_{3/2}$ units in this compound. Compared to the apical P atom in P_4S_3, the presence of the terminal sulfur group in P_4S_{10} produces a reversal in the sign of the chemical

shift anisotropy: The direction along the C_3 axis is the most shielded one.

Close inspection of the crystal structure[7,8] reveals, that the local environments of all four P atoms within the adamantanoid structure of P_4S_{10} differ slightly from each other, with Δ values of 0.9 (P-1), 2.0 (P-2), 2.4 (P-3), and 0.4 (P-4), respectively. These inequivalencies manifest themselves in the complicated multiplicity of the spectrum obtained at 11.74 T, which represents an unresolved ABCD pattern. However, the comparison of the spectra obtained at 121.65 and 202.49 MHz indicates that the main splitting observed is due to a chemical shift difference. Following a similar chemical shift asymmetry argument as for P_4S_3 above, we assign the resonance centered at 51.6 ppm to the more symmetric P(1) and P(4) sites, and the resonance centered at 49.7 ppm to P(2) and P(3), respectively.

$\underline{P_4S_9.}$ As indicated in Figure 1c, P_4S_9 contains three fourfold and one three-fold coordinated P-atom. The MAS-NMR spectrum of this compound is shown in Figure 4. The spectrum consists of five resonances (with associated spinning sidebands), four of which are characterized by a chemical shift tensor with approximately the same orientation and sign of the chemical shift anisotropy as o. served in P_4S_{10}. Therefore all of these resonances are assigned to the $S=PS_{3/2}$ sites. Field dependent spectra confirm that three of these peaks (at 64.0, 61.6, and 59.2 ppm) are visibly split by S-P-S homonuclear spin-spin coupling with a coupling constant of 80±5 Hz.

Although the NMR spectra were obtained on the disordered phase, for which no detailed crystallographic information is available, we will discuss the NMR results in terms of the known local environments present in P_4S_9-II, assuming that the S-P-S angles within the molecular cages are similar in both crystal modifications. The local environments of the three $S=PS_{3/2}$ units in the P_4S_9 molecule are all different from each other and show moderate deviations from C_{3v} symmetry (Δ values of 1.9, 2.2, 2.2, respectively). Presumably due to the disorder present in the material used in our NMR study, we can discern four instead of three ^{31}P resonances for these units. However, because of sideband

intensity distortions due to excessive peak overlap, the Herzfeld-Berger analysis could only be carried out for the peak at 67.8ppm. The peak centered at 57.7 ppm, which, together with its associated spinning sidebands, accounts roughly for 1/4 of the overall absorption, is assigned to the $PS_{3/2}$ unit. The corresponding asymmetry parameter is close to one, which is well-accounted for by the extremely distorted local environment around this phosphorus atom ($\Delta = 11.7°$), as shown in the crystal structure[10].

We note that the assignment given above agrees with that of the solution-state NMR spectrum, but is opposite to the one arrived at by Andrew and coworkers on the sole basis of relative centerband intensities[23].

P_4S_7. The molecular structure of P_4S_7 shows two three-coordinated P atoms with P-P bonds and two $S=PS_{3/2}$ units ($\Delta = 5.5$ and 7.1, respectively). The liquid-state NMR spectrum shows two singlets which had previously remained unassigned due to the lack of two-bond scalar coupling between these phosphorus atoms. Figure 5 shows the ^{31}P MAS-NMR spectrum of P_4S_7. In contrast to the liquid state NMR spectrum, in the solid state three different chemical environments are distinct, ging rise to major peak patterns centered at 82.0, 95.8, and 112.3 ppm. The integrated area ratio of these peaks including the overall spinning sideband pattern is 1:1:2. Studies at two different field strengths (see Figure 6) reveal that the multiplicity of the peak centered at 112.3 ppm arises from chemical shift differences (two major peaks at 112.8 and 111.9 ppm), whereas the splitting of the peaks centered at 82.0 and 95.8 ppm arises from homonuclear J-coupling. The corresponding coupling constant of 232 Hz is typical for a P-P single bond.[33] Thus, both resonances are assigned to the three-coordinated P-atoms, whereas the peaks at 112.8 and 111.9 ppm must be assigned to the $S=PS_{3/2}$ units. Our results and conclusions agree completely with the recent solid-state COSY study of this compound by Bjorholm.[19] Figures 4 and 5 reveal that, in contrast to the situation in liquid solution,[17] the two three-coordinated P-atoms in P_4S_7 are chemically inequivalent, resulting in a 13 ppm chemical shift difference. This difference can be understood from the crystal

structure of this material, which shows different bond angle distributions for P(1) and P(2), respectively.[6,8] The lack of further peak multiplicity for the resonances of P(1) and P(2) indicates that the two-bond spin-spin coupling constant between three- and four-coordinated P atoms remains close to zero, as it is in the liquid state.

Figure 4 shows that for the resonances due to P(1) and P(2) the intensities of the center- and spinning sidebands are unsymmetrically distributed between the two components of the spin-spin coupling pattern. Effects of this kind have been observed by Harris et al. in the ^{13}C NMR spectrum of the *ipso* carbon atom in dimethyldiphenylphosphonium iodide.[34] The combined effect of direct heteronuclear dipole-dipole interactions and chemical shift anisotropies results in a solid-state powder pattern composed of two subspectra, corresponding to the spin orientation quantum state of the P atom (+1/2 or -1/2). Slow magic-angle spinning would normally result in a sideband pattern forming the envelope of the overall powder pattern, were it not for the presence of additional scalar coupling, which allows separate observation of these subspectra. The MAS-NMR spectrum shown in Figure 4 represents an interesting example for the case of homonuclear spin-spin coupling in an AB system.

The unequal distribution of sideband intensities complicates the extraction of chemical shift tensor components from the spinning sideband patterns, especially since the angle between the principal axis of the shielding tensor and the P-P bond is not known. On the other hand, the simulations carried out by Harris and coworkers indicate that, regardless of this angle, the shapes of both subspectra will start approaching each other, if $\partial_{33}-\partial_{11}$ (in Hz) ≥ 4.5 D, where D is the dipolar coupling constant, given in our homonuclear case by

$$D = 3\gamma^2\hbar/8\pi^2r^3$$

i.e. if the difference between the most shielded and the least shielded principal component (in Hz) exceeds the dipolar coupling

constant by a factor of 4.5 or more. Using a P-P bond length of 2.33 Å from the crystal structure,[8] we calculate D to be 2340 Hz. The overall breadth of the spinning sideband pattern observed for P(1) and P(2) is ca.160 ppm, i.e. 19500 Hz at 7.05 T and 32500 Hz at 11.74 T. Thus, the error associated with a Herzfeld-Berger type analysis is expected to be relatively small, assuming that the *contribution of the anisotropy of the indirect spin-spin coupling to the spinning sideband pattern intensities is also negligible.* The chemical shift tensor components extracted by taking the peak height averages of each multiplet are listed in Table I. Our approximation appears to be justified by the observation that the shift tensor values at both field strengths used are identical within ±8ppm, albeit outside experimental error. The tensors of both P(1) and P(2) are characterized by large asymmetry parameters.

The crystal structure of P_4S_7 also indicates differences in the local environments for the four-coordinated P-atoms, which are, however, much less pronounced than for P(1) and P(2). Nevertheless, *the inequivalencies between P(3) and P(4) result in a visibly split NMR line.* Analysis of the spinning sideband intensities associated with the P(3) and P(4) resonances indicates that the chemical shift tensor of the $S=PS_{3/2}$ unit in P_4S_7 has entirely lost its axial symmetry. This is readily understood from the crystal structure which shows very large variations of S-P-S bond angles within the cages for both P(3) and P(4). The resulting geometric distortions lead to both increased overall chemical shift anisotropies, as well as a strong asymmetry of the shift tensor.

Discussion and Conclusions

The present study illustrates the power of solid state NMR in providing anisotropic chemical shift information, which is not available in the liquid state. $S=PS_{3/2}$ and $PS_{3/2}$ units with point symmetries close to C_{3v} are easily distinguished by the spinning sideband patterns revealing axially symmetric chemical shift tensors with opposite orientations: The $S=PS_{3/2}$ units are most strongly shielded along their C_{3v} axes, whereas that orientation is the most de-shielded one in $PS_{3/2}$ units. Distortions from C_{3v} symmetry manifest themselves in a loss of axial symmetry of the chemical shift tensors. Figure 7 shows a proposed correlation of the resulting asymmetry parameter with the variability of the S-P-S bond angles within the molecular cages of these compounds. In this plot, the assignment uncertainties for crystallographically inequivalent sites of a specific unit in a given compound are not shown; rather the figure assumes larger Δ values to be associated with larger asymmetry parameters. Due to different degrees of distortions observed for both the $S=PS_{3/2}$ and $PS_{3/2}$ units, the isotropic chemical shift ranges for these microstructures overlap strongly. Thus, in phosphorus sulfide systems with unknown bond angles or distributions thereof, such microstructures cannot be identified by straightforward isotropic chemical shift comparisons. However, a close inspection of Table I shows that the variation in the S-P-S bonding angles changes primarily ∂_{33}, whereas the most shielded component ∂_{11} is virtually unaffected. This is particularly evident from the plot shown for the $S=PS_{3/2}$ units in Figure 8. Thus, in an analysis of disordered or glassy systems, the presence of such units can be inferred from a unique ∂_{11} component of ca. -50±10 ppm. Table I reveals that none of the other microstructures present in the compounds studied here will pose interferences in this spectral region. In addition, Figure 8 suggests that distribution functions for intra-cage bond angles are available from ∂_{33}. However, the latter analysis will generally only be possible if the

presence of other units, which resonate in the same spectral region, has been excluded.

The limited amount of data available for compounds containing $PS_{3/2}$ units suggests a similar conclusion as above: The most shielded shift tensor component ∂_{11} remains virtually unaffected by symmetry distortions. However, in contrast to the $S=PS_{3/2}$ units, the least shielded shift tensor component decreases with increasing symmetry distortion, leading to a reduction of the overall chemical shift anisotropy. Further work on the different modifications of P_4S_4 and P_4S_5 is in progress in order to elucidate whether the ∂_{11} tensor component is sufficiently unique to enable a distinction from microstructures that may contain additional phosphorus-phosphorus bonds.

The present work suggests the utility of the anisotropic shielding information preserved in magic-angle spinning sideband patterns for making structural assignments. The approach taken here differs from the usual approach of emphasizing the isotropic chemical shift information by either fast spinning or sideband suppression techniques. We propose to use this method to identify microstructures in disordered systems such as the non-oxide chalcogenide glasses. Such studies are currently underway in our laboratories.

Acknowledgments

References

[1] Forthmann, A.; Schneider, A.; Z. Phys. Chem. , Neue Folge, 1966, 49, 22.

[2] Moedritzer, K.; Van Wazer, W.R.; J. Inorg. Nucl. Chem. 1963, 25, 683.

[3] Vincent, H.; Vincent-Forat, C.; Bull. Soc. Chim. France 1973, 499.

[4] Treadwell, W.; Beeli, Ch.; Helv. Chim. Acta 1935, 18, 1161.

[5] Kennedy, J. H.; Zhang, Z. Solid State Ionics, in press.

[6] Muller-Warmuth, W.; Eckert, H. Phys. Rep. 1982, 88, 91.

[7] Vos, A.; Wiebenga, E. H. Acta Crystallogr. 1955, 8, 217.

[8] Vos, A.; Othof, R.; Van Bolhuis, F.; Botterweg, R. Acta Crystallogr. 1965, 19, 864 .

[9] Hilmer, W. Acta Crystallogr. 1969, B 25, 1229.

[10] Leung, Y.C.; Wazer, J.; Van Houten, S.; Vos, A.; Wiegers, G. A.; Wiebenga, E. H.; Acta Crystallogr. 1957, 10, 574 .

[11] Chattopadhyay, T. K.; May, W.; Von Schnering, H. G.; Pawley, G.S.; Z. Krist. 1983 165, 47.

[12] Dixon, D. T.; Einstein, F. W. B.; Penfold, B. R.; **Acta Crystallogr.** 1965, 18, 221.

[13] Barieux, J. J.; Demarcq, M.C.; J. Chem. Soc. Chem. Commun. 1982, 177.

[14] Heckmann, G.; Fluck, E.; Z. Naturforsch., Teil B, 1971, 26, 982.

[15] Thamm, R.; Heckmann, G.; Fluck, E.; Phosphorus Sulfur 1982, 12, 319

[16] Gutowsky, H. S.; McCall, D. W.; J. Chem. Phys. 1954, 22, 162.

[17] Brevard, C; Demarcq, M.; Chem. Phys. Lett. 1981, 82, 167.

[18] Thamm, R.; Heckmann, G.; Fluck, E.; Phosphorus Sulfur 1981, 11, 273

[19] Kolditz, L.; Wahner, E.; Z. Chem. 1972, 12, 389.

[20] Jasinski, A. Magnetic Resonance and Related Phenomena, Proc. XVII Congr. Ampere (1973), 367.

[21] Andrew, E. R.; Hinshaw, W. S.; Jasinski, A. Chem. Phys. Lett. 1974, 24, 399.

[22] Andrew, E. R.; Wynn, V. T.; Proc. Roy. Soc. A 1966, 291, 257.

[23] Andrew, E. R.; Vennart, W.; Bonnard, G.; Choisnet, R. M.; Demarcq, M.; Mathieu, E.; Chem. Phys. Lett. 1976, 43, 317

[24] Bjorholm, T.; Chem. Phys. Lett. 1988, 143, 259.

[25] Gibby, M. G.; Pines, A; Rhim, W. K.; Waugh, J. S.; J. Chem. Phys. 1972, 56, 991.

[26] Taki, T.; Phys. Status Solidi. (b) 1978, 86, K147.

[27] Zumbulyadis, N.; Dailey, B. P.; Chem. Phys. Lett. 1974, 26, 273.

[28] Lucken E. A.; Williams, D. F.; Mol. Phys. 1969, 16, 17.

[29] Maricq M. M.; Waugh, J. S.; J. Chem. Phys. 1979, 70, 3300.

[30] Herzfeld, J.; Berger, A. E.; J. Chem. Phys. 1980, 73, 6021.

[31] Meisel, M.; Grunze, H.; Z. Anorg. Allg. Chem. 1970, 373, 265.

[32] Demarcq, M. C.; Phosphorus Sulfur 1981, 11, 65.

[33] Tattershall, B. W.; J. Chem. Soc. Dalton Trans. 1987, 1515.

[34] Harris, R. K.; Packer, K. J.; Thayer, A. M.; J. Magn. Reson. 1985, 62, 284.

Compound	∂_{11}^a	∂_{22}^a	∂_{33}^a	∂_{iso}^b		unit	assigt.[c]
α-P_4S_3	236	30	7	91.0	0.11	$PS_{3/2}$	P(4')
	240	14	0	84.5	0.06	$PS_{3/2}$	P(4)
P_4S_7	177	76	35	95.8	0.41	$PS_{2/2}P_{1/3}$	P(1)
	158	82	6	81.9	1.0	$PS_{2/2}P_{1/3}$	P(2)
	248	137	-49	111.9	0.60	$S=PS_{3/2}$	P(3)
	267	115	-44	112.8	0.96	$S=PS_{3/2}$	P(4)
P_4S_9	113	57	1	57.7	1.0	$PS_{3/2}$	P(4)
	139	104	40	67.8	0.24	$S=PS_{3/2}$	P(1-3)
				64.0		$S=PS_{3/2}$	d
				61.6		$S=PS_{3/2}$	d
				59.9		$S=PS_{3/2}$	d
P_4S_{10}	106	106	-57	51.6	0.0	$S=PS_{3/2}$	P(1,4)
	110	94	-55	49.7	0.11	$S=PS_{3/2}$	P(2,3)

[a]in ppm vs. 85% H_3PO_4, ±5 ppm
[b]in ppm vs. 85% H_3PO_4, ±0.1 ppm
[c]tentative assignments, based on the assumed relationship between
and Δ (see text).
[d]assignment complicated by disorder

Table I. Chemical shift tensor components (in ppm vs. 85% H_3PO_4) for crystalline phosphorus sulfides.

Figure Captions.

<u>Figure 1:</u> Molecular structures of the phosphorus sulfides under study. The atomic numbering coincides with the numbering in Table I.

<u>Figure 2:</u> 121.65 MHz ^{31}P MAS-NMR spectrum of α-P_4S_3. Spinning speed 3.3 kHz, pulse length 6 μs, recycle delay 5 min, 8 scans. Centerbands are indicated by asterisks.

<u>Figure 3:</u> 202.49 MHz ^{31}P MAS-NMR spectrum of P_4S_{10}. The inset shows the centerband region. Spinning speed 4.5 kHz, pulse length 4 μs, recycle delay 10 min, 4 scans.

<u>Figure 4:</u> 121.65 MHz ^{31}P MAS-NMR spectrum of P_4S_9. The inset shows the centerband region. Spinning speed 5.3 kHz, pulse length 7 μs, recycle delay 3 min, 12 scans.

<u>Figure 5:</u> 202.49 MHz ^{31}P MAS-NMR spectrum of P_4S_7. Spinning speed 4.2 kHz, pulse length 4 μs, recycle delay 10 min, 4 scans. Centerbands are indicated by asterisks.

<u>Figure 6:</u> Frequency dependent spectra of the centerband region of P_4S_7. The respective frequencies are indicated in the figure. Centerbands are indicated by asterisks.

<u>Figure 7:</u> Proposed correlation of the asymmetry parameter with Δ(S-P-S), the range of intra-cage bond angles. ■: S=$PS_{3/2}$ units, . ●: $PS_{3/2}$ units. In compounds with several distinct sites, tentative assignments have been made assuming the validity of this correlation. The datapoint [4.3,0.38] reflects a preliminary assignment for P_4S_5 (work in progress). The solid curve is a guide to the eye.

<u>Figure 8:</u> Correlation of the chemical shift tensor components ∂_{11}, ∂_{22}, and ∂_{33} assigned to S=$PS_{3/2}$ units with Δ(S-P-S), the range of intra-cage bond angles. The validity of the correlation of Figure 7 has not been assumed here. Therefore, the rectangles reflect assignment uncertainties to distinct sites within the structure of a given compound. Solid lines are guides to the eye.
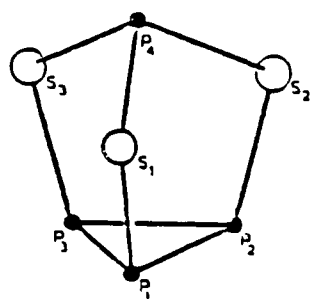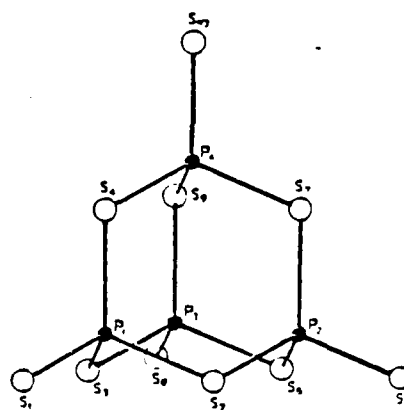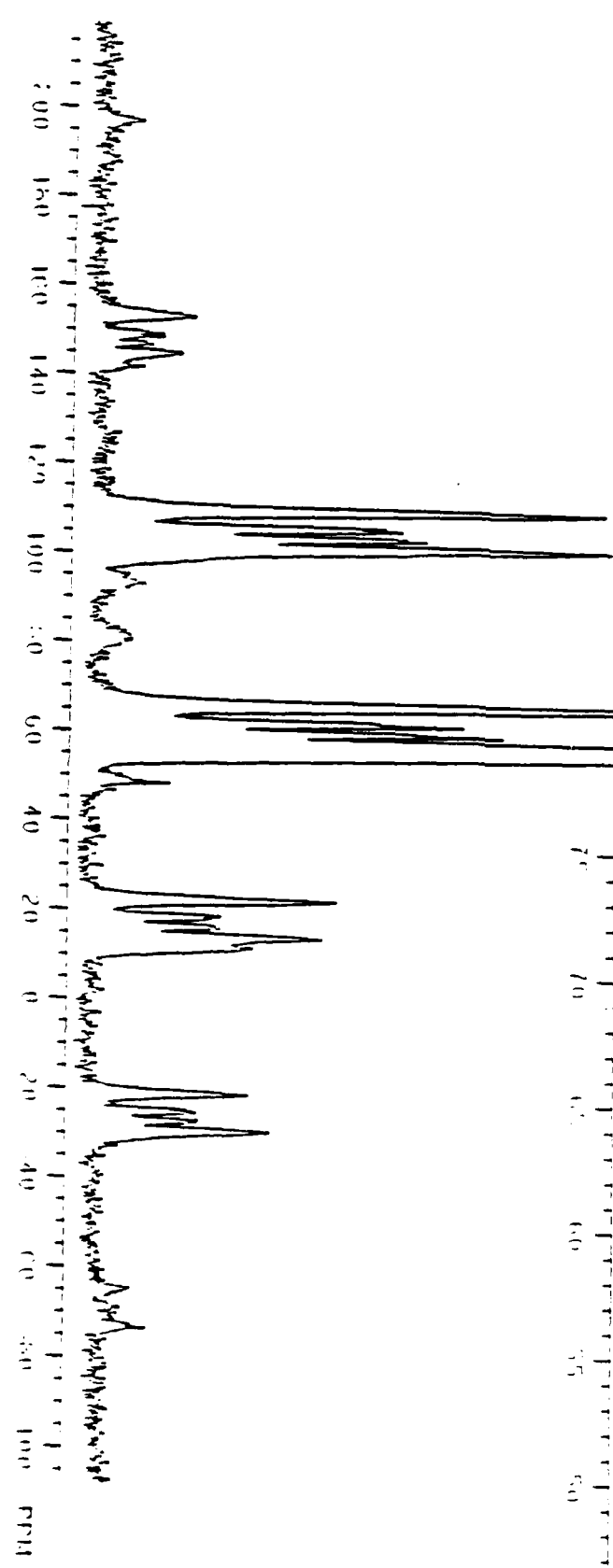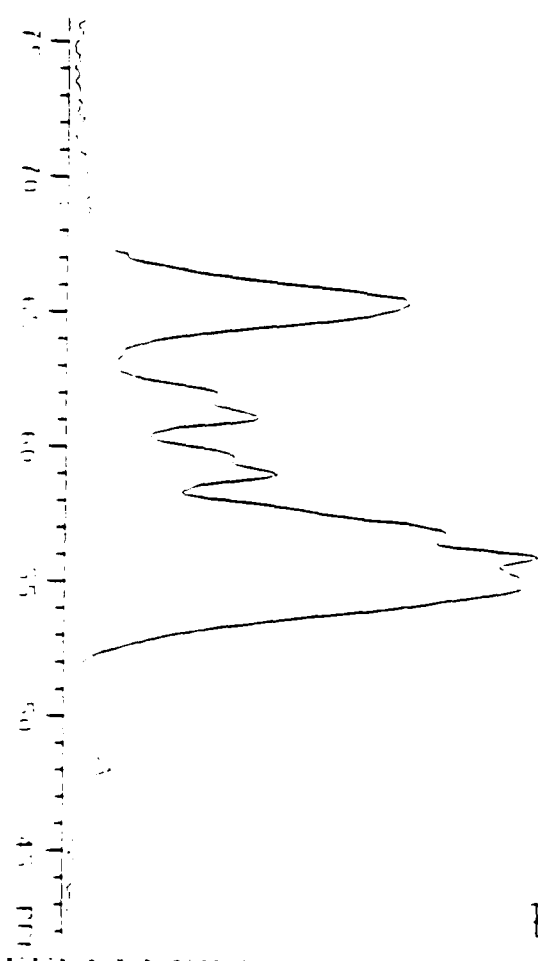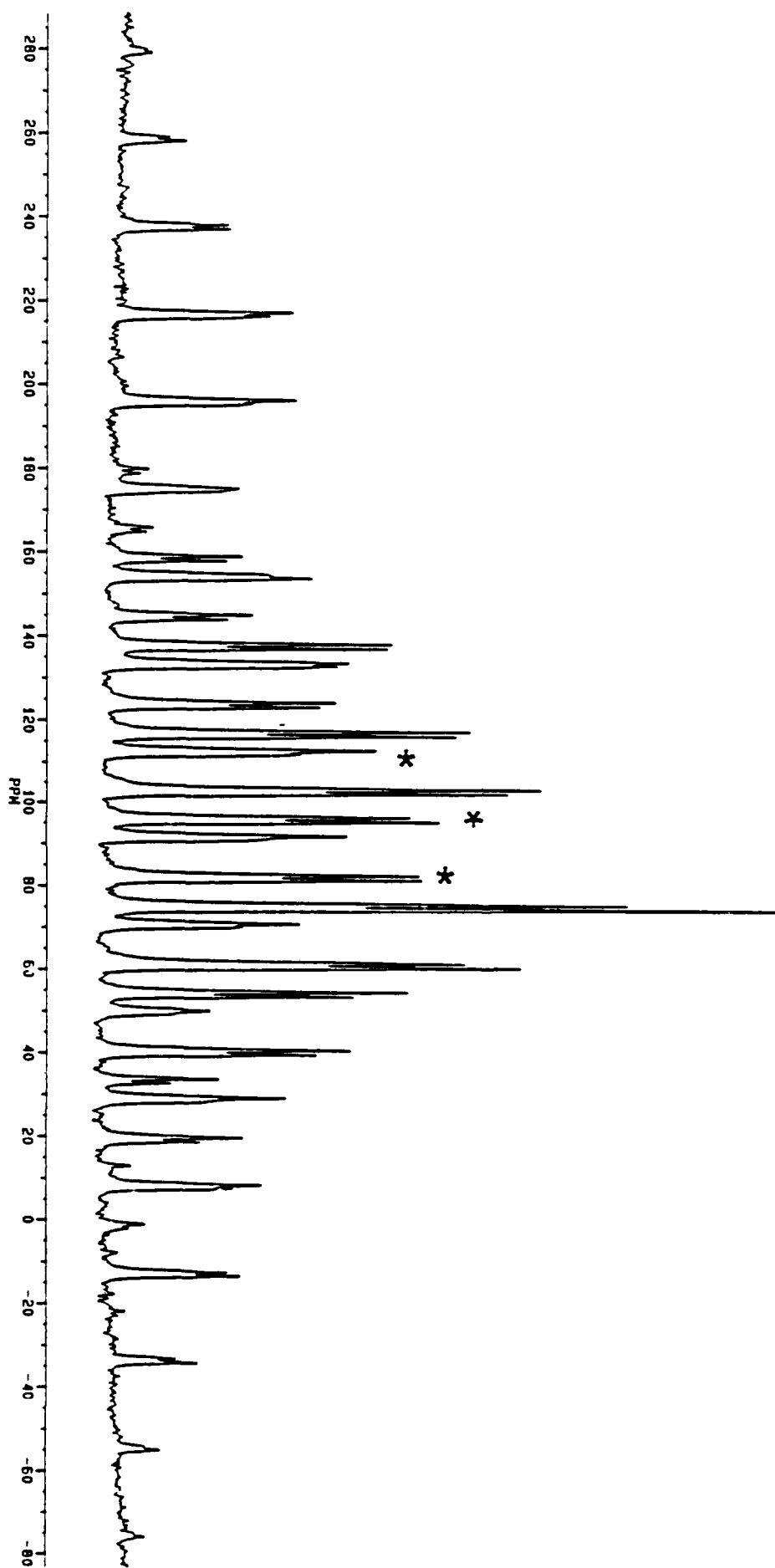
P_4S_3
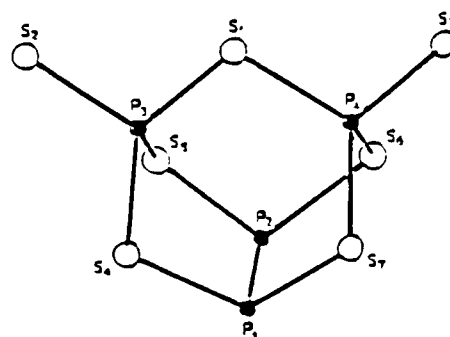
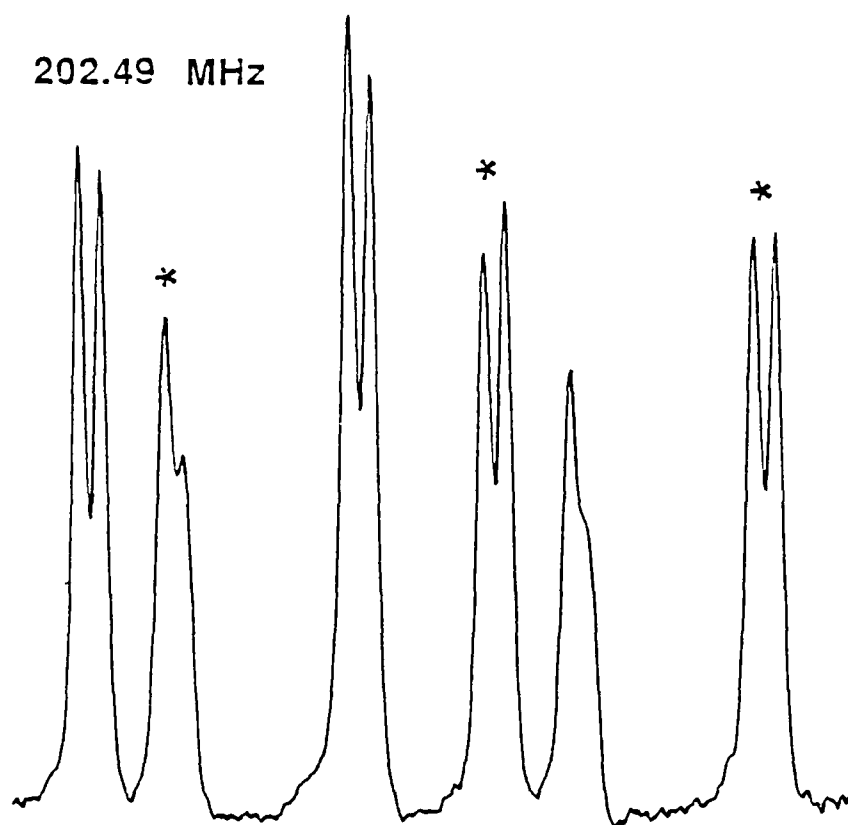P_4S_7

P_4S_9

P_4S_{10}

Fig.1

Fig. 2

Fig. 3

Fig. 4
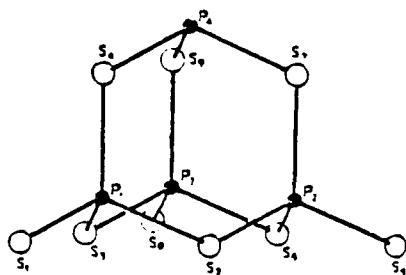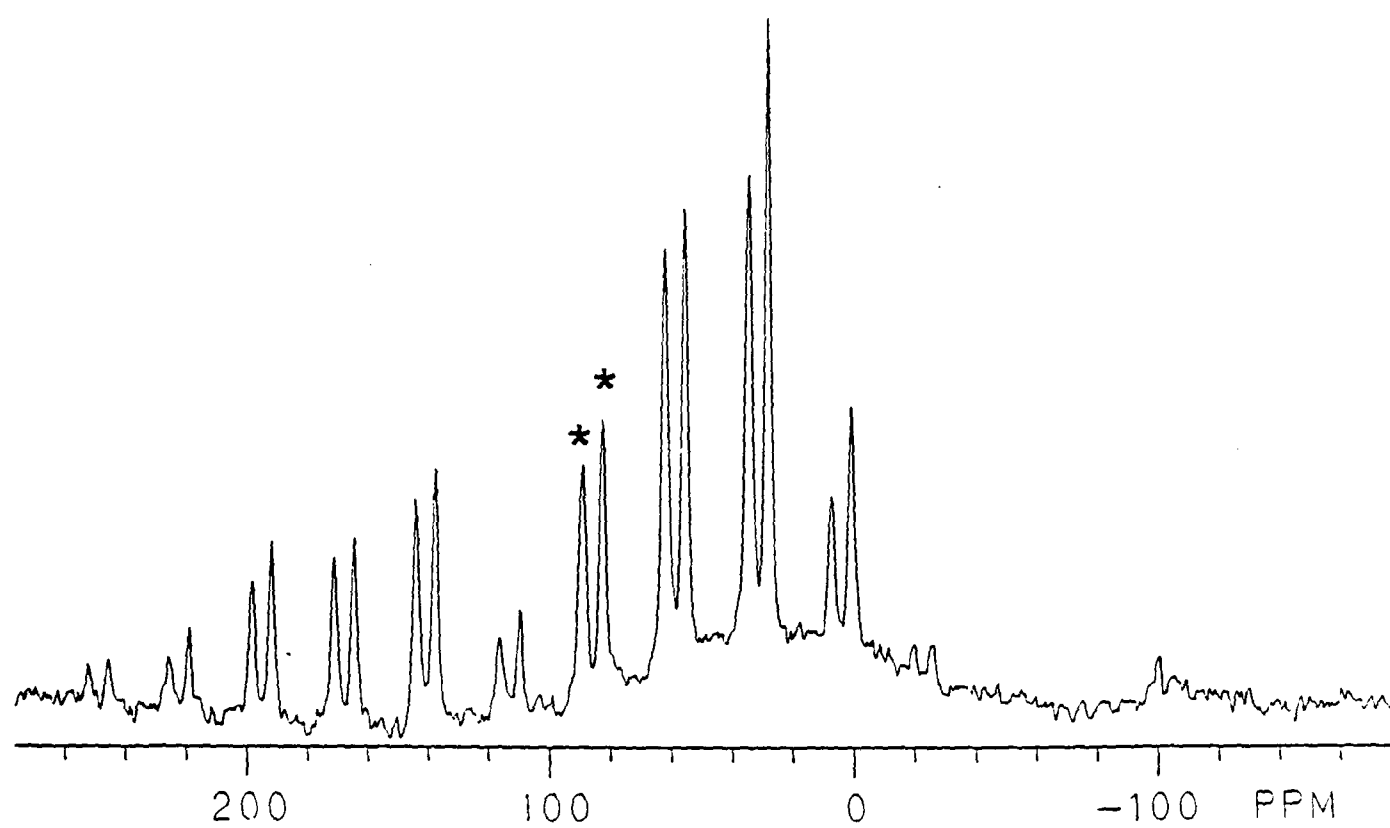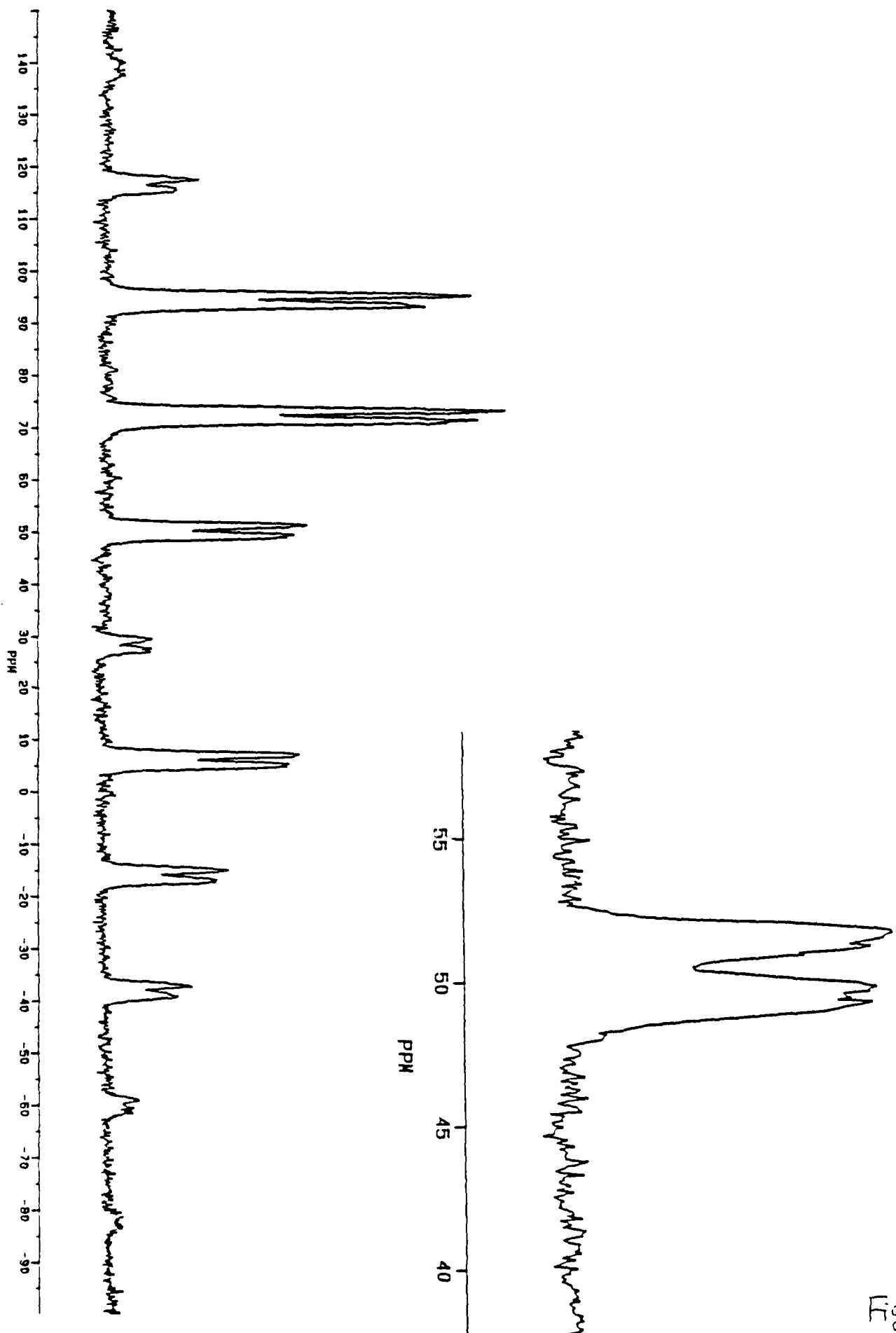
Fig.5

202.49 MHz

121.65 MHz

Fig. 6

Fig. 7

Fig. 8